International Journal of Electrical and Computer Engineering (IJECE)
Vol. 16, No. 2, April 2026, pp. 791~805
ISSN: 2088-8708, DOI: 10.11591/ijece.v16i2.pp791-805

Virtual decomposition with time delay control for underactuated robot manipulator

Imane Cheikh[1], Khaoula Oulidi Omali [2], Hachmia Faqihi[3], Mohammed Benbrahim[1], Mohammed Nabil Kabbaj[1]
[1]LIMAS Laboratory, Faculty of Sciences, Sidi Mohammed Ben Abdellah University, Fes, Morocco
[2]National School for Computer Science and Systems Analysis, Mohammed V University, Rabat, Morocco
[3]SETIME Laboratory, Ibn Tofail University, Kenitra, Morocco

Article Info

Article history:

Received Aug 2, 2025
Revised Dec 26, 2025
Accepted Jan 16, 2026

Keywords:

Co-simulation
Nonlinear control
Time delay estimation
Underactuated robot manipulator
Virtual decomposition control

ABSTRACT

The importance of controlling robot manipulators is undeniable. However, faults in these systems can significantly impact the workspace environment and personal safety. To address these challenges, a new adaptive approach has been proposed that easily adapts to a faulty actuator while precisely tracking its desired position. The virtual decomposition control (VDC) method decomposes the robot into subsystems, each with its sub-controller, while ensuring the overall system remains stable. Meanwhile, time delay estimation (TDE) is used to estimate unknown and uncertain parameters. A co-simulation was conducted to test the TD-VDC method on a 6 DoFs robot, which becomes underactuated during its running. The results of the root main square error of the proposed controller were lower of 6% than those of sliding mode control based on partial feedback linearization control (SMC-PFLC), which proves the proposal's effectiveness and efficiency.

Corresponding Author:

Imane Cheikh
LIMAS laboratory, Faculty of Sciences, Sidi Mohammed Ben Abdellah University
Fes, Morocco
Email: imane.cheikh@usmba.ac.ma

1. INTRODUCTION

In many recent applications, manipulator robots have become a key production tool in modern industry [1], [2]. However, the likelihood of unintentional actuator failures remains present at any stage of the robot's lifecycle, continuously exposing the controller to the risk of losing its stability and effectiveness. Therefore, controlling underactuated robot manipulators for tracking trajectories effectively has gained significant attention and become more challenging [3]. In such cases, we are dealing with underactuated robots, which have a greater number of degrees of freedom (DoFs) than active actuators, transforming their dynamic system into a nonlinear complex problem. To mitigate this challenge, a redundant controller is required to maintain the system's stability whenever an actuator fault occurs [4]. To achieve this, a new controller for the underactuated robot is proposed in this paper, enabling the robot to perform its tasks and become resilient to actuator faults.

To address this issue, the literature has proposed various methods to control underactuated robots, which can be generally grouped into different categories. Robust methods such as sliding mode control [5], [6], passivity-based control [7], and backstepping control [8] are known for their robustness against disturbances and parameter variations. However, they are sensitive to chattering phenomena and become more complex when an actuator fault occurs. Traditional controllers or their submerging are widely used, such as partial feedback linearization control [9], and many others [10]. Yet, they are not sufficiently robust

to handle model uncertainties and faults. Intelligent controllers are also used to control underactuated robots, such as fuzzy control [11], neural network control [12], data-driven proportional-integral-derivative (DD-PID) [13]. Nevertheless, some of these methods require training, others depend on the presence of data and optimization algorithms. Moreover, combining controllers can also enhance the performance of the merged controller, like sliding mode control based on fuzzy logic and neural networks [14], nonfragile prescribed performance control [15] and the super-twisting control method with improved potential energy function [16], which are all known for their robustness. However, many of the control methods mentioned below are established using the Lagrange-Euler dynamic model. Therefore, those methods are based on one dynamic equation that regroups all the joints together. So, whenever an actuator fault occurs in one joint, it can affect the control of all the other joints. Furthermore, adapting this model to the underactuated systems introduces significant complexity due to the need for various parameters and for some controllers, the need for data and optimization, which leads to high control effort, time consumption, and more resources. In addition, recent advanced controllers were proposed, such as sigmoid PID [17], brain emotional learning-based intelligent controller (BELBIC) PID [18], and neuroendocrine PID [19], but they often rely on centralized architectures, heuristic tuning, or data-driven training. In the meantime, having a passive joint, unknown uncertainties, and disturbances in the system increasingly enhances the complication and the computational burden.

To manage the problems mentioned above, a new adaptive control approach based on time delay with virtual decomposition control (TD-VDC) was designed in the paper [20] to control the full-actuated robot manipulator. In contrast to the recent advanced controllers discussed earlier, the proposed TD-VDC framework offers a structured, decentralized control scheme. This approach allows each joint to be regulated independently, enhancing robustness to uncertainties and scalability. Moreover, TD-VDC avoids the need for complex optimization procedures or complete dynamic models, such as the aforementioned Euler-Lagrange approaches, making it particularly well-suited for controlling underactuated manipulators. The main idea behind the general virtual decomposition control (VDC) [21] is to decompose the robot into subsystems (link dynamics and joint dynamics). Then, each subsystem is controlled independently with a designed sub-controller while ensuring the overall system stability. In the present paper, this approach is reconfigured to suit the dynamics of the underactuated robot manipulator with an actuator fault. Therefore, this method leads to isolating and readapting the passive joint controller of the underactuated robot independently without impacting the sub-controllers of the active joints. As a result, using VDC simplifies the control of each subsystem of the underactuated robot even with defective joints. Furthermore, to define the full dynamic equation of the robot, the well-known solution is the regression method [22]. However, some of its drawbacks are the difficulty of designing the regressor matrix and handling the uncertainties and disturbances. To cope with these challenges, the time delay estimation (TDE) has proved its design simplicity and effectiveness in approximating unknown uncertainties and disturbances [23]. Thus, by merging the VDC and TDE, we establish the time delay estimation based virtual decomposition control (TD-VDC) for an underactuated robot. As a result, it presents many advantages such as design simplicity, robustness against unknown dynamics, and high precision in trajectory tracking.

Furthermore, evaluating our suggested controller on the manipulator robot through co-simulation replicates the actual robot's behavior before deploying the controller on physical hardware. This approach simplifies the process of inducing joint defects into the underactuated robot, allowing more effective observation of the robot's performance. Consequently, co-simulation testing of the controller helps identify the best solution for the situation at hand.

The present paper provides a deeper understanding of the importance of the proposed approach in controlling an underactuated manipulator. Section 1 describes the dynamic system of an n-DoF underactuated manipulator with an i^{th} defective joint. Subsequently, the proposed controller based on TD-VDC is adapted to a robot manipulator with passive joints in section 2. Then, section 3 proves the stability analysis for the controller TD-VDC. In section 4, a case of a 6-DoF underactuated manipulator with a defective actuator is performed via a co-simulation with MATLAB and Simulink. Moreover, a comparison analysis is discussed between the results of TD-VDC and sliding mode control based on partial feedback linearization control (SMC-PFLC). Finally, the conclusions are established in section 5.

2. THE PROPOSED METHOD

2.1. Underactuated system description

The underactuated manipulator robot is a complex dynamic system with a higher number of degrees of freedom than active joints. Based on the Euler-Lagrange approach, the n-link underactuated manipulator robot is characterized as follows, with a_p representing passive joints, a_1 and a_3 being active joints, and the total number of joints satisfying the equation $a_1 + a_p + a_3 = n$ joints, as mentioned in [10]:

$$M_u \begin{pmatrix} \ddot{q}_{a1} \\ \ddot{q}_{ap} \\ \ddot{q}_{a3} \end{pmatrix} + \begin{pmatrix} C_{a1}\dot{q}_{a1} \\ C_p\dot{q}_{ap} \\ C_{a3}\dot{q}_{a3} \end{pmatrix} + \begin{pmatrix} G_{a1} \\ G_{ap} \\ G_{a3} \end{pmatrix} = \begin{pmatrix} \tau_{a1} \\ 0_{ap} \\ \tau_{a3} \end{pmatrix} + \begin{pmatrix} \tau_{d_{a1}} \\ \tau_{d_{ap}} \\ \tau_{d_{a3}} \end{pmatrix}; \quad (1)$$

With q_{aj}, $\dot{q}_{aj}$, $\ddot{q}_{aj} \in \Re^{aj}$ with $j = \{1, p, 3\}$ are the vectors of the initial active, the passive, and the last active joints' positions, velocities, and accelerations; $M_u(q) \in \Re^{n \times n}$ is the underactuated robot inertia matrix, and it is divided into 6 sub-matrices; C_{aj}=$C(q, \dot{q})_{aj}\dot{q}_{aj} \in \Re^{aj}$ gather the initial, the passive, and the last active vectors of the Coriolis and centripetal torques; G_{aj} =$G(q)_{aj} \in \Re^{aj}$ denote the gravitational torques vector; $\tau_{a1} \in \Re^{a1}$ and $\tau_{a3} \in \Re^{a3}$ are the first and the last input torque vectors applied to the joints, while $0_{ap} \in \Re^{ap}$ is a vector of zeros that is applied to the passive joint and $\tau_{d_{aj}} \in \Re^{aj}$ present the disturbance vector.

2.2. System decomposition

Similar to a full-actuated manipulator control, the virtual decomposition of an n-DoF underactuated robot with an i^{th} passive joint is defined by splitting the links and the joints. Figure 1 shows the representation of the virtual decomposition of an underactuated robot based on the one for the full-actuated robot shown in the paper [21]. The cutting point associated with frames *{B_i},* and *{T_{i+1}}* is related to the i^{th} link, while the cutting point associated with frames *{B_i},* and *{T_i}* is related to the i^{th} joint.

To control the underactuated robot, each subsystem, including the *n* links, the *n* joints, and the passive joint, will be treated independently. To do so, we will need to define the required velocities before expressing the link and joint dynamics equations. Then, the global system dynamic equation will be computed by adding individual joints and links torques.

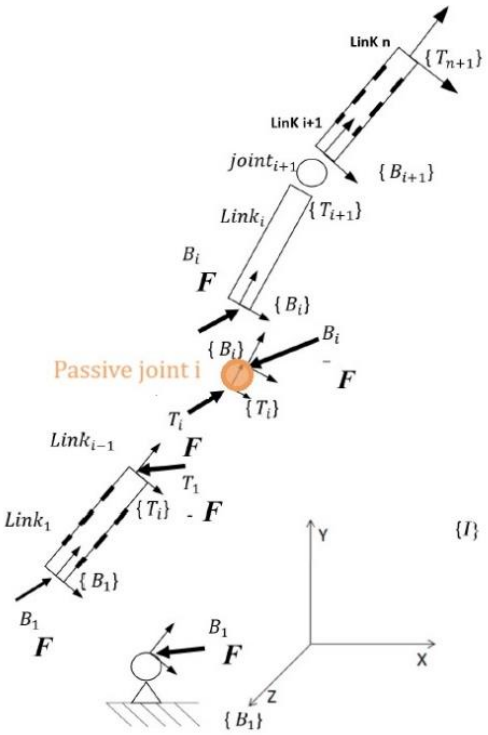

Figure 1. Virtual decomposition of an underactuated manipulator

2.2.1. Required velocities

Required velocities are one of the most important concepts in designing the VDC controller for the underactuated robot. They are calculated based on the joint position error and desired velocity. Therefore, they allow the robot to adhere to the desired trajectory with high precision. Based on the paper [21], the equations below are introduced.

On the one hand, we can express the i^{th} joint required velocity that can be active or passive:

$$\dot{q}_{i,r} = \dot{q}_{i,d} - \gamma\,(error_i); \quad (2)$$

Where $q_{i,d}, \dot{q}_{i,d}$ are the i^{th} goal joint position and velocity; q_i is the i^{th} real joint position and $error_i = q_{i,d} - q_i$.

On the other hand, the i^{th} link required linear/angular velocity is computed in (3):

$$^{B_i}V_r = z\dot{q}_{id} - {}^{B_{i-1}}U_{B_i}{}^{T}\,{}^{Bi-1}V_r\,; \tag{3}$$

Where $z = [0\ 0\ 0\ 0\ 0\ 1]^T$ for revolute joint and the transformation matrix ${}^{B_{i-1}}U_{B_i}$ from the frame $\{B_{i-1}\}$ to the frame $\{B_i\}$ is expressed as:

$$\begin{aligned} {}^{B_{i-1}}U_{B_i} &= \begin{pmatrix} {}^{B_{i-1}}R_{B_i} & 0_{3\times3} \\ \left({}^{B_{i-1}}r_{B_i}\times\right){}^{B_{i-1}}R_{B_i} & {}^{B_{i-1}}R_{B_i} \end{pmatrix}; \\ \left({}^{B_{i-1}}r_{B_i}\times\right) &= \begin{pmatrix} 0 & -{}^{B_{i-1}}r_{B_i}(3) & {}^{B_{i-1}}r_{B_i}(2) \\ {}^{B_{i-1}}r_{B_i}(3) & 0 & -{}^{B_{i-1}}r_{B_i}(1) \\ -{}^{B_{i-1}}r_{B_i}(2) & {}^{B_{i-1}}r_{B_i}(1) & 0 \end{pmatrix}; \end{aligned} \tag{4}$$

Where ${}^{B_{i-1}}R_{B_i}$ is the rotation Matrix and ${}^{B_{i-1}}r_{B_i}$ is the vector of transformation from the frame $\{B_{i-1}\}$ to the frame $\{B_i\}$.

2.2.2. Links dynamics

Using the required linear/angular velocity in (3), the equation of the required net moment vector ${}^{B_i}F_r^{*}$ that is exerted by the ith-1 link on the ith link is expressed as following the paper [21]:

$$^{B_i}F_r^{*} = M_{B_i}\frac{d^{B_i V_r}}{dt} + C_{B_i}{}^{B_i}V_r + G_{B_i}; \tag{5}$$

Where M_{B_i} is the inertial term, C_{B_i} is the centrifugal and Coriolis term, G_{B_i} represents the gravitational term.

Iteratively, we can find the generalized moment ${}^{B_i}F_r$ applied from the i^{th+1} body on the i^{th} body with the following expression as defined in the paper [21]:

$$\begin{aligned} {}^{Bn}F_r &= {}^{Bn}F_r^{*}; \\ {}^{Bn-1}F_r &= {}^{Bn-1}F_r^{*} + {}^{Bn-1}U_{Bn}\,{}^{Bn}F_r^{*}; \\ &\vdots \\ {}^{Bi-1}F_r &= {}^{Bi-1}F_r^{*} + {}^{Bi-1}U_{B_i}\,{}^{B_i}F_r^{*};\ for\ i=[2,\ldots,n-1] \end{aligned} \tag{6}$$

Finally, the required net torque of the i^{th} joint toward the links is computed with the use of (6):

$$\tau_{il,r} = z^{T}\,{}^{B_i}F_r; \tag{7}$$

2.2.3. Joints dynamics

Based on the joint required velocity in (2), the i^{th} joint subsystem dynamic is expressed with the equation of the required net torque $\tau_{ij,r}$ as follows, as mentioned in the paper [21]:

$$\tau_{ij,r} = I_{mi}\ddot{q}_{i,r} + \xi_{ci}sign(\dot{q}_{i,r}); \tag{8}$$

Where I_{mi} is the moment of inertia and $\xi_{ci}$is the i^{th} Coulomb friction coefficient.

2.2.4. System dynamics

By combining the expressions in (7) and (8), we find that the total torque for an n-DoF robot is as described in the paper [21]:

$$\tau_i = \tau_{ij,r} + \tau_{il,r}; \tag{9}$$

In this section, the joints' and links' dynamics for a robot manipulator have been expressed using the virtual decomposition control. The next step is to design the new controller for the underactuated robot with a passive joint. Therefore, a new control law will be proposed in the next section to define the VDC for an underactuated robot manipulator.

3. METHOD

3.1. Proposed controller for underactuated manipulator TD-VDC

As already described in section 2, the joints and links' using the VDC for a full-actuated manipulator robot have been mentioned. In order to adapt this controller to the underactuated dynamics, a new control law is designed in the following theorem for the underactuated robot based on the system decomposition. Then, the new controller is proven.

Theorem 1: By integrating the control law for the underactuated robot expressed in (1), with the total torque for a full-actuated manipulator robot, the new control torque input for the n-DoF underactuated manipulator with p passive joints is designed as (10):

$$\begin{pmatrix} \tau_{a1} \\ 0_{ap} \\ \tau_{a3} \end{pmatrix} = \begin{pmatrix} \tau_{a1j,r} + \tau_{a1l,r} \\ \tau_{apj,r} + \tau_{apl,r} \\ \tau_{a3j,r} + \tau_{a3l,r} \end{pmatrix}; \quad (10)$$

Where $\tau_{a1j,r} \in \Re^{a1}$ and $\tau_{a3j,r} \in \Re^{a3}$ are the first and the last required net torque vectors applied to the joints; $\tau_{a1l,r} \in \Re^{a1}$ and $\tau_{a3l,r} \in \Re^{a3}$ are the first and the last active required net torque applied to the links; $\tau_{apl,r}, \tau_{apj,r} \in \Re^{ap}$ are the passive required net torques applied to links and joints respectively. From (10), we deduce the new key concept in controlling underactuated robots with p passive joints based on VDC and which can be represented as (11):

$$\tau_{apl,r} = -\tau_{apj,r}; \quad (11)$$

Proof: The underactuated robot is characterized by having fewer joint actuators than DoFs. As the dynamic (1) mentions, the passive joint exerts a null torque that cannot be controlled. Therefore, the total torque for the underactuated robot can be categorized into active and passive torques, represented as τ_{a1}, τ_{a3} for the active joints and 0_{ap} for the passive ones.

$$\tau = \begin{pmatrix} \tau_{a1} \\ 0_{ap} \\ \tau_{a3} \end{pmatrix}; \quad (12)$$

By referring to (9) and (12), we can derive Theorem 1 concerning the virtual decomposition control of the underactuated robot. The main results of the theorem are given in (10) and (11). These results will be used in the subsequent sections.

While VDC presents significant advantages in controlling underactuated manipulators, challenges remain in ensuring robustness against external disturbances and uncertainties in system dynamics. To tackle these challenges, the concept of TDE is introduced to account for dynamic uncertainties. This enhancement leads to the proposed TD-VDC approach, which significantly improves both stability and control efficiency for underactuated manipulators with passive joints. The overall model for controlling the underactuated manipulator based on TD-VDC is outlined in Figure 2, which illustrates the corresponding block diagram.

By separating the dynamics of the links and joints in (10) from Theorem 1, the new approach integrates the (5) and (8) of VDC along with the estimation of TDE as already given in paper [20]. Then the equations for links and joints are as:

For links:

$$\begin{aligned} {}^{Ba1}F_r^{*} &= \overline{m_{a1}}\,{}^{Ba1}\dot{V}_r + \hat{L}_{a1,l} + K_{a1,l}\,{}^{Ba1}e_l; \\ {}^{Bap}F_r^{*} &= \overline{m_{ap}}\,{}^{Bap}\dot{V}_r + \hat{L}_{ap,l} + K_{ap,l}\,{}^{Bap}e_l; \\ {}^{Ba3}F_r^{*} &= \overline{m_{a3}}\,{}^{Ba3}\dot{V}_r + \hat{L}_{a3,l} + K_{a3,l}\,{}^{Ba3}e_l; \end{aligned} \quad (13)$$

For joints:

$$\begin{aligned} \tau_{a1j,r} &= \overline{\iota_{m,a1}}\ddot{q}_{a1,r} + \hat{L}_{a1,j} + K_{a1,j}\,{}^{a1}e_j; \\ \tau_{apj,r} &= \overline{\iota_{m,ap}}\ddot{q}_{ap,r} + \hat{L}_{ap,j} + K_{ap,j}\,{}^{ap}e_j; \\ \tau_{a3j,r} &= \overline{\iota_{m,a1}}\ddot{q}_{a3,r} + \hat{L}_{a3,j} + K_{a3,j}\,{}^{a3}e_j; \end{aligned} \quad (14)$$

Where $\overline{m_k}, \overline{\iota_{m,k}}$ $with\ k = [a1, ap, a3]$ are constants associated with the inertial term and the moment of inertia; $\hat{L}_{k,c}$ $with\ c = [l, j]$ refer to the estimated vectors of the unknown dynamic uncertainties and

disturbances $F_{k,c}$ of link' and active/passive joint' systems; ${}^{Bk}e_l = {}^{Bk}V_r - {}^{Bi}V$ defines the tracking accuracy error; ${}^{k}e_j = \dot{q}_{k,r} - \dot{q}_k$ defines the tracking joint error; And $K_{k,c}$ are positive gains.

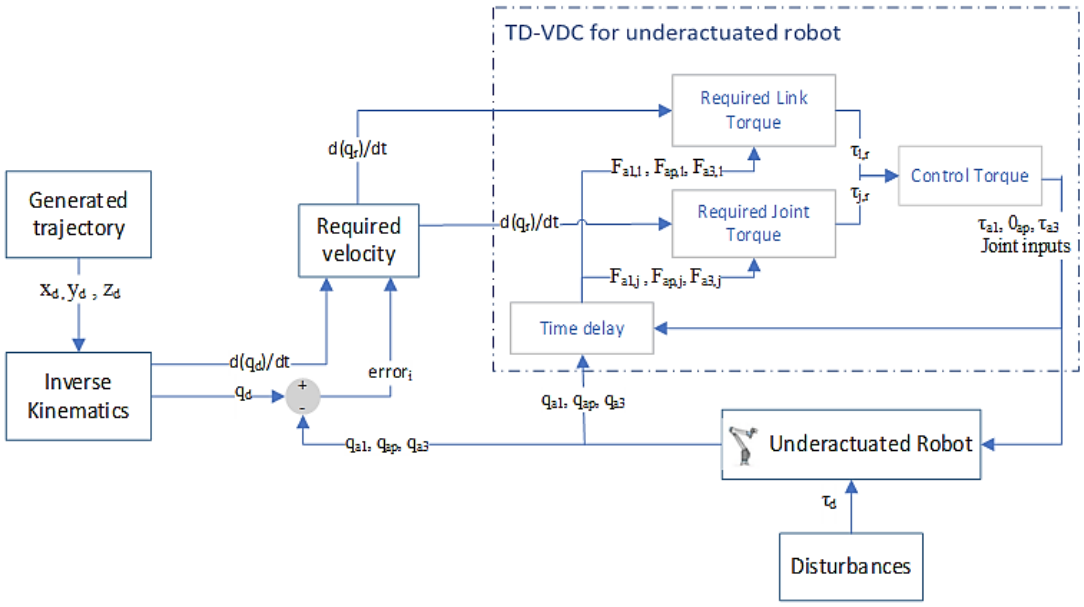

Figure 2. Block diagram of the underactuated manipulator's control

To ensure the stability of the proposed controller, we make the following assumptions:

a. S1: the vectors $L_{k,c}$ and their derivatives are global Lipschitz functions. Consequently, their values at the present time *(t)* and at the past time *(t-T)* are nearly equal with *T* as a low time delay:

$$\hat{L}_{k,c}(t) = \hat{L}_{k,c}(t-T); \tag{15}$$

b. S2: The constants $\overline{m_k}$ and $\overline{\iota_{m,k}}$ are picked so that:

$$\begin{aligned} \left|I_n - M(q)\overline{m_k}^{-1}\right| < 1 \\ \left|I_n - I(q)\overline{\iota_{m,k}}^{-1}\right| < 1 \end{aligned} \tag{16}$$

For simplification, let us consider an n-DoF underactuated robot with the p[th] joint as a passive joint. Then, we find links' subsystems based on (15), (13) and (11):

$$\begin{aligned} \hat{L}_{n,l}(t) &= [z\,\tau_{nl,r}(t-T) - \overline{m}_n\,{}^{Bn}\dot{V}(t-T) - \\ &\quad K_{n,l}\,{}^{Bn}e_l(t-T)]; \\ &\vdots \\ \hat{L}_{p,l}(t) &= [-z\,\tau_{pj,r}(t-T) - \overline{m}_p\,{}^{Bp}\dot{V}(t-T) - \\ &\quad K_{p,l}\,{}^{Bp}e_l(t-T) - {}^{Bp}U_{Bp+1}(t-T)\hat{L}_{p+1,l}(t-T) + \\ &\quad \overline{m}_{p+1}\,{}^{Bp+1}\dot{V}(t-T) + K_{p+1,l}\,{}^{Bp+1}e_l(t-T)]; \\ &\vdots \\ \hat{L}_{i,l}(t) &= [z\,\tau_{il,r}(t-T) - \overline{m}_i\,{}^{Bi}\dot{V}(t-T) - \\ &\quad K_{i,l}\,{}^{Bi}e_l(t-T) - {}^{Bi}U_{Bi+1}(t-T)\hat{L}_{i+1,l}(t-T) + \\ &\quad \overline{m}_{i+1}\,{}^{Bi+1}\dot{V}(t-T) + K_{i+1,l}\,{}^{Bi+1}e_l(t-T)\,]; \end{aligned} \tag{17}$$

The above equations show that the $\hat{L}_{p,l}(t)$ is related directly to the passive joint torque $\tau_{pj,r}$ which has a big impact on adjusting the controller. Furthermore, we remark that all the estimations before one of the passive joints $\hat{L}_{p,l}$ are related to the latter estimation. This implies that the torque control of the links before the passive joint adapts easily whenever a fault occurs. Similarly, we find for joints subsystems:

$$\begin{aligned} \hat{L}_{n,j}(t) &= \tau_{nj,r}(t-T) - K_{n,j}{}^{n}e_j(t-T); \\ &\vdots \\ \hat{L}_{i,j}(t) &= \tau_{ij,r}(t-T) - K_{i,j}{}^{i}e_j(t-T); \end{aligned} \tag{18}$$

Therefore, based on the (6), (7), (11), (13), (14), (17), and (18), the proposed controllers for n-DoF underactuated robot with a p^{th} joint unactuated are divided into two categories:

- For active joint:

$$\begin{aligned} \tau_{il,r} &= \tau_{il,r}(t-T) + z^T[\overline{m_i}\Delta({}^{B_i}\dot{V}_r) + K_{i,l}\Delta({}^{B_i}e_l) + \overline{m_{i+1}}{}^{B_{i+1}}\dot{V}(t-T) + K_{i+1,l}{}^{B_{i+1}}e_l(t-T) + \\ &\quad \Delta({}^{B_i}U_{B_{i+1}}\hat{L}_{i+1,l}) + {}^{B_{i-1}}U_{B_i}(\overline{m_{i+1}}{}^{B_{i+1}}\dot{V}(t) + K_{i+1,l}{}^{B_{i+1}}e_l(t))]; \\ \tau_{ij,r} &= \overline{I_{m,i}}\ddot{q}_{i,r} + \tau_{ij,r}(t-T) + K_{i,j}\Delta({}^{i}e_j); \end{aligned} \tag{19}$$

- For passive joint:

$$\begin{aligned} \tau_{pl,r} &= -\tau_{pl,r}(t-T) + z^T[\overline{m_p}\Delta({}^{B_p}\dot{V}_r) + K_{p,l}\Delta({}^{B_p}e_l) + \overline{m_{p+1}}{}^{B_{p+1}}\dot{V}(t-T) + \\ &\quad K_{p+1,l}{}^{B_{p+1}}e_l(t-T) + \Delta\left({}^{B_p}U_{B_{p+1}}\hat{L}_{p+1,l}\right) + \\ &\quad {}^{B_{p-1}}U_{B_p}(\overline{m_{p+1}}{}^{B_{p+1}}\dot{V}(t) + K_{p+1,l}{}^{B_{p+1}}e_l(t))]; \\ \tau_{pj,r} &= \overline{I_{m,p}}\ddot{q}_{p,r} + \tau_{pj,r}(t-T) + K_{p,j}\Delta({}^{p}e_j); \end{aligned} \tag{20}$$

With $\Delta(X) = X(t) - X(t-T)$ is the TDE error [22].

Subsequently, the control torques are derived by adding the joint and link torques in (19) and (20) as shown in Theorem 1. The next step is to demonstrate the stability of the controller to prove its effectiveness. Then, the new control torques will be used to control the underactuated robot with a passive joint.

3.2. TD-VDC stability analysis

To prove the system's stability per Theorem 1, a non-negative total Lyapunov candidate V_T is defined. Two non-negative Lyapunov candidates are summed up, the first one for links V_{il} and the second one for joints V_{ij}. It is expressed as follows for $i = \{1, \ldots, p, \ldots, n\}$ [21]:

$$V_T = \sum_{i=1}^{n} V_{il} + \sum_{i=1}^{n} V_{ij}; \tag{21}$$

With:

$$\begin{aligned} V_{il} &= \frac{1}{2}{}^{B_p}e_l{}^{T}M_{B_I}{}^{B_p}e_l + \frac{1}{2}\left(L_{i,l} - \hat{L}_{i,l}\right)^2 \\ V_{ij} &= \frac{1}{2}I_{m,i}{}^{i}e_j{}^{2} + \frac{1}{2}\left(L_{i,j} - \hat{L}_{i,j}\right)^2 \end{aligned} \tag{22}$$

Then by deriving each Lyapunov candidate, we have:

$$\begin{aligned} \dot{V}_{il} &= -{}^{B_i}e_l{}^{T}K_{i,l}{}^{B_i}e_l + {}^{B_i}e_l{}^{T}\left({}^{B_{ai}}F_r{}^{*} - {}^{B_{ai}}F^{*}\right) + \Delta\left(L_{i,l}\right)\left(Y_i{}^{T}{}^{B_i}e_l - \frac{1}{2T}\Delta\left(L_{i,l}\right)\right) \\ \dot{V}_{ij} &= -K_{i,j}{}^{i}e_j{}^{2} + {}^{i}e_j(\tau_{ij,r} - \tau_{ij}) + \frac{1}{2T}\Delta\left(L_{i,j}\right)^2 \end{aligned} \tag{23}$$

Where Y_i is a term used in the regression method.

As mentioned above, $L_{k,c}$ is a global Lipschitz function, which means that:

$$\left|\Delta\left(L_{k,c}\right)\right| \leq \partial_{kc}T \quad with\ \partial_{kc} > 0 \tag{24}$$

However, it is necessary to define the virtual power flows concerning frame A as [21]:

$$p_A = {}^{A}e_l{}^{T}({}^{A}F_r - {}^{A}F) \tag{25}$$

Accordingly, this leads to finding the total virtual power for an open chain structure, as we have a manipulator robot:

$$\sum_{i=1}^{n}(p_{B_i} - p_{T_i}) = \sum_{i=1}^{n} {}^{B_i}e_l^{\,T}({}^{B_i}F_r^{\,*} - {}^{B_i}F^{*}) = 0 \tag{26}$$

According to (22), (23), (24), and (26), we obtain the total Lyapunov candidates as:

$$\begin{aligned} \sum_{i=1}^{n}\dot{V}_{il} &\leq -\sum_{i=1}^{n}({}^{B_i}e_l^{\,T}K_{i,l}{}^{B_i}e_l + \tfrac{1}{2}\partial_{il}) \\ \sum_{i=1}^{n}\dot{V}_{ij} &\leq -\sum_{i=1}^{n}(K_{i,j}{}^{i}e_j^{\,2} + \tfrac{1}{2}\partial_{ij}) \end{aligned} \tag{27}$$

However, the Lipschitz constants $\partial_{il}, \partial_{ij}$ and the gains $K_{i,l}, K_{i,j}$ are strictly positive as mentioned in (23). Therefore, the stability of the closed-loop system is proved since $\dot{V}_T$ is a negative-definite function:

$$\begin{aligned} \dot{V}_T &= \sum_{i=1}^{n}\dot{V}_{il} + \sum_{i=1}^{n}\dot{V}_{ij} \\ \dot{V}_T &< 0 \end{aligned} \tag{28}$$

The finite-time convergence of the VDC with time delay can be given by integrating the Lyapunov candidate:

$$\int_0^{t_c}\dot{V}_T \leq -\sum_{i=1}^{n}\int_0^{t_c}({}^{B_i}e_l^{\,T}K_{i,l}{}^{B_i}e_l + \tfrac{1}{2}\partial_{il}) - \sum_{i=1}^{n}\int_0^{t_c}(K_{i,j}{}^{i}e_j^{\,2} + \tfrac{1}{2}\partial_{ij}) \tag{29}$$

By considering that ${}^{B_i}e_l(t_c) = {}^{i}e_j(t_c) \cong 0$, we deduce:

$$V_{il}(t_c) + V_{ij}(t_c) - V_{il}(0) - V_{ij}(0) \leq \tfrac{1}{3}K_{i,l}{}^{B_i}e_l^{\,3}(0) - \tfrac{1}{2}(\partial_{ij} + \partial_{il})t_c + \tfrac{1}{3}K_{i,j}{}^{i}e_j^{\,3}(0) \tag{30}$$

From (15), (16), and (23), we have $V_{il}(t_c) = V_{ij}(t_c) \cong 0$. Then, we replace them in (30) with their expression from (22):

$$t_c \leq \frac{2}{\partial_{il}+\partial_{ij}}(\tfrac{1}{2}{}^{B_i}e_l^{\,T}(0)\overline{m_l}{}^{B_i}e_l(0) + \tfrac{1}{3}K_{i,l}{}^{B_i}e_l^{\,3}(0) + \tfrac{1}{2}\overline{\iota_{m,\iota}}{}^{i}e_j^{\,2}(0) + \tfrac{1}{3}K_{i,j}{}^{i}e_j^{\,3}(0)) \tag{31}$$

Hence, the above result guarantees a convergence time based on TD-VDC approach less short than the expression given in (31).

In this section, the new TD-VDC for the underactuated robot has been developed and its stability has been proved. To test its effectiveness, a case study is introduced in the next section using the robot manipulator UR10. In order to test the underactuated controller, a joint fault is co-simulated using MATLAB and Simulink.

4. RESULTS AND DISCUSSION

4.1. Case study description

To illustrate the effectiveness of the proposed control strategy, this section presents a case study performed for tracking trajectory, in Cartesian space, using the UR10 robotic manipulator [24]. The intended joint angles are obtained by converting the desired end-effector position using inverse kinematics [25]. The manipulator robot is considered a full-actuated robot. However, it transitions to an underactuated state when the fifth joint experiences a fault. To address this, the discussed TD-VDC controller is designed based on the model developed in sections 2 and 3, and the robot model is co-simulated in Mechanics Explorer, using MATLAB and Simulink Software. The full-actuated UR10 has 6 DoFs, while the considered underactuated UR10 has a fifth passive joint, with the remaining joints remaining active. The real values for the passive joint q5 are obtained directly from the co-simulation used with Simulink.

To perform the proposed controller, the robot is initially fully-actuated and is controlled using the TD-VDC. However, when an actuator fails at a chosen time, the robot becomes underactuated. In this situation, the designed controller switches automatically to the underactuated TD-VDC mode, which applies Theorem 1. The simulation model is developed using MATLAB and Simulink as shown in Figure 3, which corresponds to the block diagram shown in Figure 2.

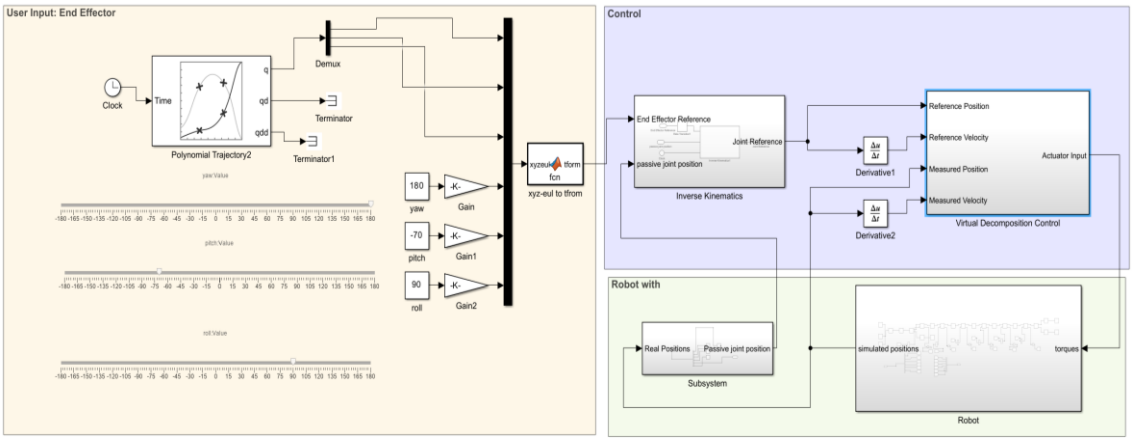

Figure 3. The TD-VDC co-simulation setup

As depicted in Figure 3, the user input block defines the desired trajectory, depending on each application's requirements. The control block corresponds to the inverse kinematics module, whose outputs are fed into the robot controller to compute the joint torques. The robot block represents the simulated robot, which uses these torques and performs the tracking trajectory. When a joint failure occurs, the passive joint position is then incorporated into the inverse kinematics model.

This co-simulation aims to track a desired position trajectory in cartesian space with the full-actuated UR10. Thereafter, the fifth joint becomes passive at *t=2s.* In the same way as a pick-and-place industrial trajectory, the end-effector desired positions $p_{d,k} = \{x_{d,k}, y_{d,k}, z_{d,k}\}$ with $k = [0, \dots, 4]$ start from an initial goal position and go to four goal positions, respectively, in different desired times of arrival t_{kf} and velocities $\dot{p}_{\mathrm{d,k}}$. Herein, we choose to use the cubic polynomial trajectory [26]:

$$p_{d,k}(t) = a_3(t-t_0)^3 + a_2(t-t_0)^2 + a_1(t-t_0) + a_0; \quad (32)$$

Where $a_0 = p_{d,0}$, $a_1 = \dot{p}_{d,0}$, $a_2 = \frac{3}{{t_{kf}}^2}\left(p_{d,\mathrm{k}} - p_{d,0}\right) - \frac{2}{t_{kf}}\dot{p}_{d,0} - \frac{1}{t_{kf}}\dot{p}_{d,k}$, and $a_3 = \frac{2}{{t_{kf}}^3}\left(p_{d,\mathrm{k}} - p_{d,0}\right) - \frac{1}{{t_{kf}}^2}\left(\dot{p}_{d,0} + \dot{p}_{d,k}\right)$ are the coefficients of the cubic polynomial trajectory. The physical parameters of the manipulator robot UR10 are described in Table 1 [27]. Those parameters are used in TD-VDC calculations.

Table 1. Physical parameters of the UR10 robot

Mass (Kg)	Length (m)	Coulomb friction coefficient (N.m)	Moment of inertia (Kg.m^2)
m_1=7.778	l_1=0.1273	$\xi_{c1} = 0.5$	$i_{m,1}$ =0.04201
m_2 = 12.930	l_2=0.6120	$\xi_{c2} = 0.5$	$i_{m,2}$ =1.6143
m_3 = 3.870	l_3=0.5723	$\xi_{c3} = 0.5$	$i_{m,3}$ =0.4225
m_4 = 1.960	l_4=0.1639	$\xi_{c4} = 0.5$	$i_{m,4}$ =0.0175
m_5 = 1.960	l_5=0.1157	$\xi_{c5} = 0.5$	$i_{m,5}$ =0.0087
m_6 = 0.202	l_6=0.0922	$\xi_{c6} = 0.5$	$i_{m,6}$ =0.0005

Moreover, we inject the uncertainties and disturbances at all the tracking trajectory times as:

$$\tau_d(t) = \begin{cases} e^{-5t} * sin(2t) \\ cos(2t) \\ cos(2t) \\ 0 \\ 0 \\ 0 \end{cases} \quad (33)$$

Following the closed-loop block diagram given in Figure 2, we use a time delay equal to the fixed sample time $T_s = 10^{-4}$(s). This choice enhances accuracy and precision during real-time simulation in Simulink. Furthermore, the constants $\overline{m_k}, \overline{I_{m,k}}$ are chosen according to assumption S2. No formal optimization or

model-based tuning was applied in this work. Due to the system's complexity and the absence of a precise analytical model, the links and joints control parameters $K_{i,l}, K_{i,j}$ were determined through a trial-and-error process. Initial gains were chosen, then refined via iterative simulations to meet the suitable performance goals in stability and trajectory tracking.

4.2. Co-simulation results

The co-simulation results are presented for the proposed TD-VDC controller and the SMC-PFLC controller developed in the paper [4] on the task space. The same trajectory is tested for both controllers to better compare the results of the controllers. Furthermore, the same uncertainties and disturbances are also taken into account as mentioned in (33).

For that purpose, Figure 4 shows two of the five real desired positions during the co-simulation, demonstrating how the UR10 effectively tracks these positions in cartesian space. Figures 5 and 6 describe the position errors for the six joints of the robot UR10 under the TD-VDC and SMC-PFLC, respectively. Figures 7(a) and 7(b) further detail the tracking trajectory in cartesian space for both controllers SMC-PFLC and TD-VDC, highlighting the performance differences. Furthermore, joints' torques change periodically with high precision due to the choice of Ts.

Moreover, Table 2 represents a comparative study between the two approaches TD-VDC and SMC-PFLC to control the robot UR10 that is full-actuated until the time $t = 2s$ and then becomes underactuated with the fifth joint passive. Additionally, the root main square (RMS) is adopted to evaluate the controllers quantitatively and is defined as:

$$RMSe(t) = \sqrt{\frac{1}{T}\int_0^T |(error_i(t)|^2 dt} \tag{34}$$

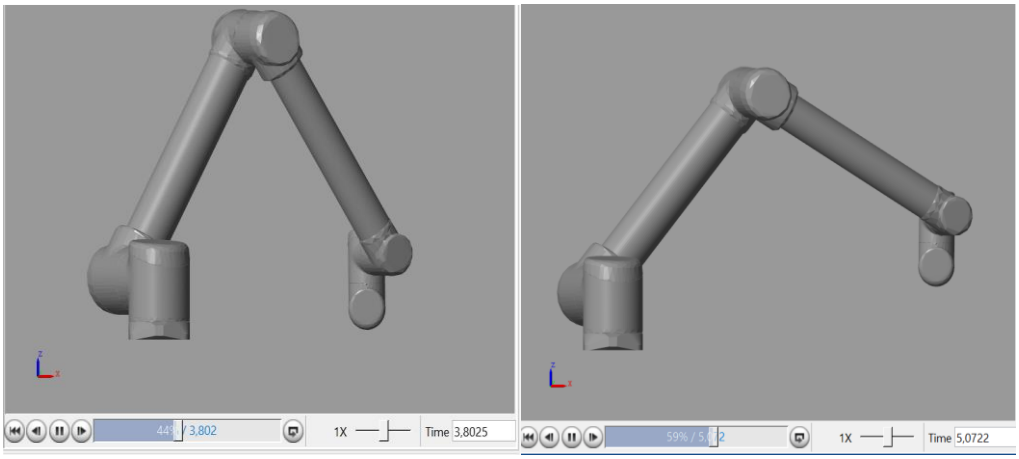

Figure 4. Two examples of co-simulated desired positions at different time scales

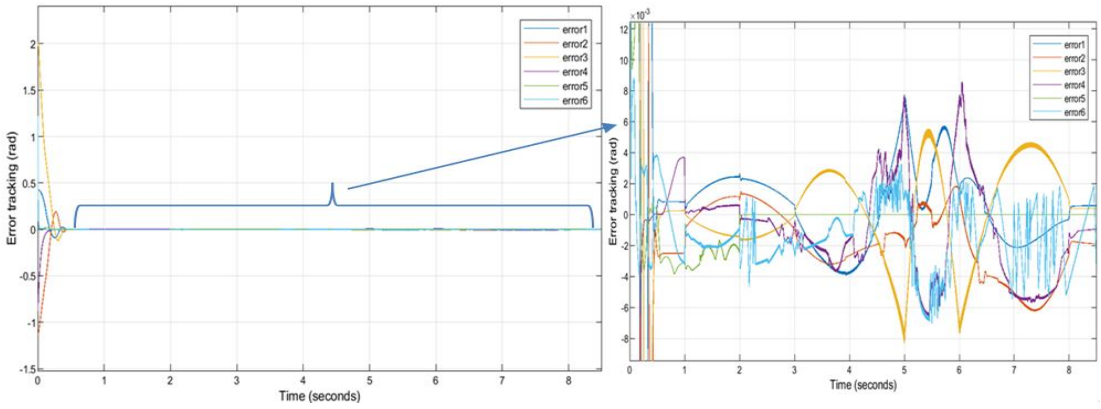

Figure 5. Error tracking using the TD-VDC for the underactuated robot UR10

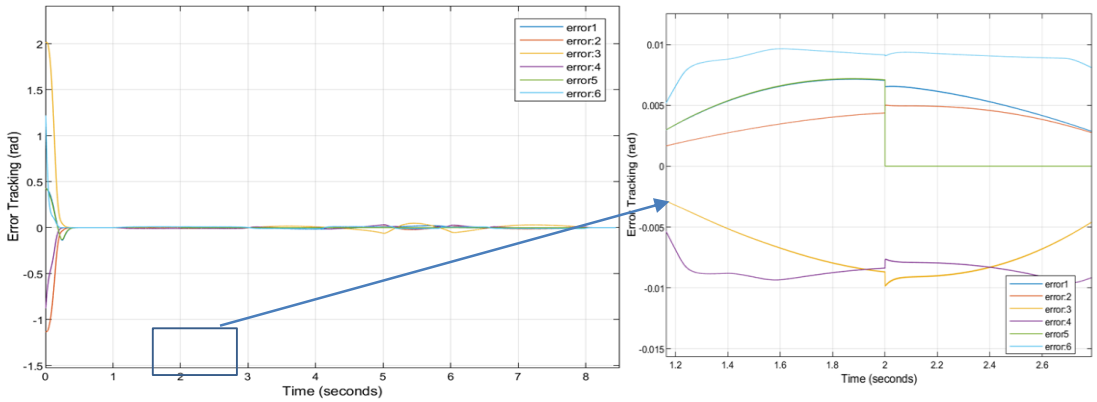

Figure 6. Error tracking using the SMC-PFLC for the underactuated robot UR10

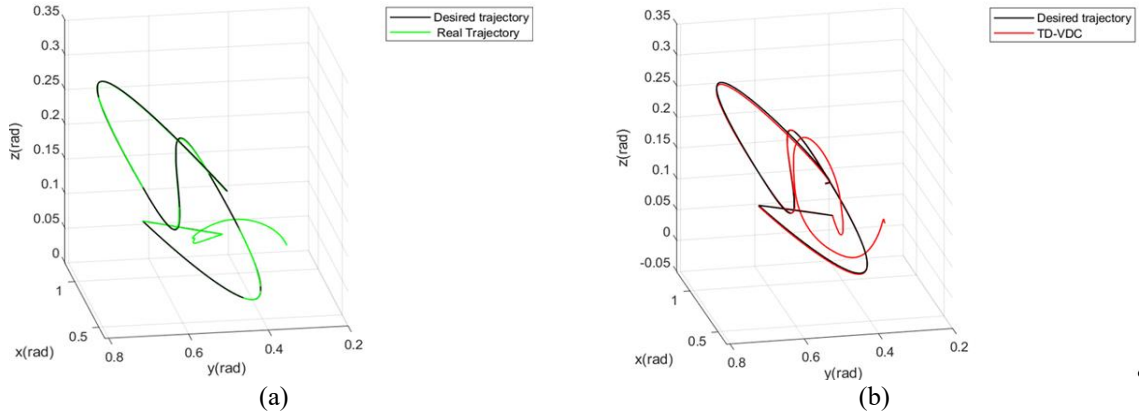

Figure 7. Cartesian trajectory tracking using (a) SMC-PFLC vs (b) TD-VDC controllers for the underactuated robot UR10

Table 2. Comparative study

Control type	Convergence time t_c (sec)	Errors (rad) for i =[1, ..., 6] and ∝>0	RMS error (rad)
TD-VDC	0.4	Max$\{error_i(t \geq t_c)\} \cong \propto .10^{-3}$	$RMSe_x$=0.081 $RMSe_y$=0.021 $RMSe_z$=0.010
SMC − PFLC	0.392	Max$\{ error_i(t \geq t_c)\} \cong \propto .10^{-2}$	$RMSe_x$=0.086 $RMSe_y$=0.023 $RMSe_z$=0.012

4.3. Results discussion

This manuscript proposes a novel control approach for underactuated robotic manipulators by combining virtual decomposition control with time delay estimation. The method enables decentralized and modular control of complex robotic systems without relying on full dynamic models. The main goal of this discussion is to explain the effectiveness and the performance of the TD-VDC to control an underactuated robot with a passive joint through co-simulation results. To do so, we chose to compare the TD-VDC approach with SMC-PFLC, which is one of the Euler-Lagrange traditional existing strategies to control an underactuated robot.

According to the presented co-simulation results, for the SMC-PFLC, we need to design two control blocks: the first for the full-actuated controller using SMC and the second for the underactuated control using SMC based on PFLC. For this methodology, the dynamic equation is based on the Euler-Lagrange model as described in (1). In order to be suitable for the underactuated robot, new changes have been performed on the dynamic equation, which affected the system's stability. Therefore, many readaptations were needed to ensure the controller's stability and the tracking trajectory's effectiveness. As a result, designing this controller is a complex and time-consuming task.

On the other hand, the TD-VDC used for the actuated robot UR10 was readapted using Theorem 1 to control the manipulator robot when an actuator fault appears at a time $t = 2s$. This new approach decomposes the dynamic systems into sub-systems of links and joints. This decomposition leads to controlling each part independently of the other parts of the underactuated robot. Therefore, the main focus was on the passive joint sub-system. As a result, the TD-VDC has proved its simplicity and adaptability while transitioning between the two controllers, the first is for the full-actuated manipulator UR10, and the second is for the underactuated manipulator UR10.

Moreover, the comparison study in Table 2 shows that the convergence time for the tested SMC-PLC controller is practically higher by 2% than for the tested TD-VDC controller. However, the TD-VDC achieves better tracking trajectory precision as its RMS error is lower by 6% than the SMC-PFLC's RMS error. Furthermore, the controlled joints of the underactuated UR10 using the TD-VDC are tracking the desired trajectory more accurately than those using the SMC-PFLC, as depicted in Figures 4 and 5. From all the results, we summarize the main differences between the two controllers in Table 3. The first column represents the main strengths of the TD-VDC for the underactuated robot manipulator. Meanwhile, the second column represents the strengths and the limitations of SMC-PFLC.

Table 3. Comparison between TD-VDC and SMC-PFLC for the underactuated robot

TD-VDC	SMC-PLFC
Robust	Robust
Simple	Complex
Adaptive to different faults	Not adaptive
Precise	Errant

To summarize, the simulation results prove the effectiveness and the robustness of the proposed controller TD-VDC in handling an actuator fault. As well as simplifying the control design for the underactuated robot, it also does not impact the active joints' controllers while maintaining an accurate trajectory tracking. However, the SMC-PFLC, which is based on the Euler-Lagrange model, needs more time and resources to implement an accurate and effective controller, and that is developing the robot parameters has an impact on the whole system control.

5. CONCLUSION

To conclude, a new methodology has been chosen to control an n-DoF underactuated manipulator with nonlinear dynamics and unknown uncertainties. The main contribution in this paper is to propose a new TD-VDC controller for a fully actuated manipulator robot that suddenly became underactuated due to a faulty joint actuator. Furthermore, the stability of the controller has been proved with the Lyapunov approach. Then, co-simulations were performed using MATLAB and Simulink for the TD-VDC and SMC-PFLC for a 6 DoFs robot that became underactuated with the 5th joint faulty at a specific time while tracking a desired trajectory to visualize the robot's behavior. The computed results showed the simplicity, adaptivity, and precision of the TD-VDC controller compared to the SMC-PFLC, whose design is more complex and less precise. Additionally, the co-simulation demonstrated that the tracking trajectory was well maintained during the transition between the full-actuated and underactuated controllers. These findings lay the groundwork for further research for testing more than one passive joint using the TD-VDC, given that each sub-controller can be tuned on its own. Furthermore, a practical implementation using a real underactuated robot in a real environment is quite challenging. In future work, the proposed controller will be tested on more complex underactuated systems with actuator and sensor faults.

FUNDING INFORMATION

Authors state no funding involved.

AUTHOR CONTRIBUTIONS STATEMENT

This journal uses the Contributor Roles Taxonomy (CRediT) to recognize individual author contributions, reduce authorship disputes, and facilitate collaboration.

Name of Author	C	M	So	Va	Fo	I	R	D	O	E	Vi	Su	P	Fu
Imane Cheikh	✓	✓	✓	✓	✓	✓	✓	✓	✓	✓			✓	
Khaoula Oulidi Omali							✓				✓			
Hachmia Faqihi		✓		✓		✓	✓			✓	✓	✓		
Mohammed Benbrahim				✓		✓				✓	✓	✓	✓	
Mohammed Nabil Kabbaj						✓					✓	✓	✓	

C : **C**onceptualization
M : **M**ethodology
So : **So**ftware
Va : **Va**lidation
Fo : **Fo**rmal analysis
I : **I**nvestigation
R : **R**esources
D : **D**ata Curation
O : Writing - **O**riginal Draft
E : Writing - Review & **E**diting
Vi : **Vi**sualization
Su : **Su**pervision
P : **P**roject administration
Fu : **Fu**nding acquisition

CONFLICT OF INTEREST STATEMENT

Authors state no conflict of interest.

DATA AVAILABILITY

Derived data supporting the findings of this study are available from the corresponding author, IC, on request.

REFERENCES

[1] Y. Zhang *et al.*, "Fault types and diagnostic methods of manipulator robots: a review," *Sensors*, vol. 25, no. 6, p. 1716, 2025, doi: 10.3390/s25061716.

[2] B. Zeng, Y. Li, X. Gong, H. Wang, Z. Huang, and H. Zhou, "Velocity trajectory planning and tracking control based on basis function superposition and metaheuristic algorithms for planar underactuated manipulators," *Actuators*, vol. 14, no. 10, p. 505, Oct. 2025, doi: 10.3390/act14100505.

[3] S. Mustary, M. A. Kashem, J. M. Sony, N. Hossain, and M. A. Chowdhury, "Advancing stability in robot manipulators: A review of recent progress and parameters," *Engineering Reports*, vol. 7, no. 7, Jul. 2025, doi: 10.1002/eng2.70207.

[4] I. Cheikh, H. Faqihi, M. Benbrahim, and M. N. Kabbaj, "Robust sliding mode based on partial feedback linearization control for underactuated robot manipulator," in *Lecture Notes in Networks and Systems*, vol. 1101 LNNS, S. Motahhir and B. Bossoufi, Eds. Springer, 2024, pp. 487–497, doi: 10.1007/978-3-031-68675-7_46.

[5] J. Liu, *Sliding mode control using MATLAB*, 1st Ed. China: Elsevier Inc, 2017.

[6] R. J. Yahya and N. H. Abbas, "Optimal integral sliding mode controller controller design for 2-RLFJ manipulator based on hybrid optimization algorithm," *International Journal of Electrical and Computer Engineering*, vol. 12, no. 1, pp. 293–302, 2022, doi: 10.11591/ijece.v12i1.pp293-302.

[7] B. Caasenbrood, A. Pogromsky, and H. Nijmeijer, "Energy-shaping controllers for soft robot manipulators through port-hamiltonian cosserat models," *SN Computer Science*, vol. 3, no. 6, p. 494, 2022, doi: 10.1007/s42979-022-01373-w.

[8] M. L. Castano and X. Tan, "Backstepping-based tracking control of underactuated aquatic robots," *IEEE Transactions on Control Systems Technology*, vol. 31, no. 3, pp. 1179–1195, 2023, doi: 10.1109/TCST.2022.3215585.

[9] M. W. Spong, S. Hutchinson, and M. Vidyasagar, *Control of underactuated systems in robot modeling and control*, 2nd ed. John Wiley \& Sons, 2020.

[10] X. Xin and Y. Liu, *Control design and analysis for underactuated robotic systems*, vol. 9781447162513. Springer, 2014, doi: 10.1007/978-1-4471-6251-3.

[11] M. Zhai, S. Diao, T. Yang, Q. Wu, Y. Fang, and N. Sun, "Adaptive fuzzy control for underactuated robot systems with inaccurate actuated states and unavailable unactuated states," *IEEE Transactions on Automation Science and Engineering*, vol. 22, pp. 1566–1578, 2025, doi: 10.1109/TASE.2024.3367921.

[12] J. Wu, J. She, Y. Wang, and C. Y. Su, "Position and posture control of planar four-link underactuated manipulator based on neural network model," *IEEE Transactions on Industrial Electronics*, vol. 67, no. 6, pp. 4721–4728, 2020, doi: 10.1109/TIE.2019.2926050.

[13] N. S. A. Shukor, M. A. Ahmad, and M. Z. M. Tumari, "Data-driven PID tuning based on safe experimentation dynamics for control of liquid slosh," *2017 IEEE 8th Control and System Graduate Research Colloquium, ICSGRC 2017 - Proceedings*, pp. 62–66, 2017, doi: 10.1109/ICSGRC.2017.8070569.

[14] Q. N. Xuan, C. N. Cong, and N. N. Ba, "Robust adaptive trajectory tracking sliding mode control for industrial robot manipulator using fuzzy neural network," *Journal of Robotics and Control (JRC)*, vol. 5, no. 2, pp. 490–499, Mar. 2024, doi: 10.18196/jrc.v5i2.20722.

[15] J. Zhang, P. Han, Z. Wu, Q. Liu, and J. Yang, "Nonfragile prescribed performance control of robot manipulators with actuator faults," *International Journal of Control, Automation and Systems*, vol. 22, no. 11, pp. 3472–3481, 2024, doi: 10.1007/s12555-024-0174-z.

[16] L. Wang, J. Hu, and M. Fu, "Distributed containment control of the underactuated vessels with collision/obstacle avoidance and connectivity maintenance," *Ocean Engineering*, vol. 298, p. 117194, Apr. 2024, doi: 10.1016/j.oceaneng.2024.117194.

[17] G. Sitaramu, L. Dutta, and D. Kumar Das, "To design sigmoid based PID controller for twin rotor MIMO system," in *2023 Second IEEE International Conference on Measurement, Instrumentation, Control and Automation (ICMICA)*, May 2024, pp. 1–5, doi: 10.1109/ICMICA61068.2024.10732610.

[18] S. Saat, M. A. Ahmad, and M. R. Ghazali, "Data-driven brain emotional learning-based intelligent controller-PID control of

MIMO systems based on a modified safe experimentation dynamics algorithm," *International Journal of Cognitive Computing in Engineering*, vol. 6, pp. 74–99, Dec. 2025, doi: 10.1016/j.ijcce.2024.11.005.
[19] M. Z. Mohd Tumari, M. A. Ahmad, M. H. Suid, M. R. Ghazali, and M. O. Tokhi, "An improved marine predators algorithm tuned data-driven multiple-node hormone regulation neuroendocrine-PID controller for multi-input–multi-output gantry crane system," *Journal of Low Frequency Noise Vibration and Active Control*, vol. 42, no. 4, pp. 1666–1698, 2023, doi: 10.1177/14613484231183938.
[20] H. Faqihi, K. Benjelloun, M. Saad, M. Benbrahim, and M. N. Kabbaj, "New time delay estimation-based virtual decomposition control for n-DoF robot manipulator," *IAES International Journal of Robotics and Automation (IJRA)*, vol. 10, no. 3, p. 192, 2021, doi: 10.11591/ijra.v10i3.pp192-206.
[21] W. H. Zhu and G. Vukovich, "Virtual decomposition control for modular robot manipulators," *IFAC Proceedings Volumes (IFAC-PapersOnline)*, vol. 44, no. 1 PART 1, pp. 13486–13491, 2011, doi: 10.3182/20110828-6-IT-1002.02233.
[22] S. Lampinen, J. Koivumaki, and J. Mattila, "Improved hydraulic cylinder model for the virtual decomposition control approach," in *Proceedings of the IEEE 2019 9th International Conference on Cybernetics and Intelligent Systems and Robotics, Automation and Mechatronics, CIS and RAM 2019*, 2019, pp. 113–118, doi: 10.1109/CIS-RAM47153.2019.9095788.
[23] J. Lee, P. H. Chang, and M. Jin, "Adaptive integral sliding mode control with time-delay estimation for robot manipulators," *IEEE Transactions on Industrial Electronics*, vol. 64, no. 8, pp. 6796–6804, 2017, doi: 10.1109/TIE.2017.2698416.
[24] P. M. Kebria, S. Al-wais, H. Abdi, and S. Nahavandi, "Kinematic and dynamic modelling of UR5 manipulator," in *2016 IEEE International Conference on Systems, Man, and Cybernetics (SMC)*, Oct. 2016, pp. 4229–4234, doi: 10.1109/SMC.2016.7844896.
[25] I. Hutama and C. H. Kuo, "Adaptive sliding mode control of a 6-DOF RLED robot manipulator with uncertain parameters and external disturbances," *International Journal of Automation and Smart Technology*, vol. 6, no. 1, pp. 13–24, 2016, doi: 10.5875/ausmt.v6i1.1026.
[26] R. Hanifi Elhachemi Amar, L. Benchikh, H. Dermeche, O. Bachir, and Z. Ahmed-Foitih, "Trajectory reconstruction for robot programming by demonstration," *International Journal of Electrical and Computer Engineering (IJECE)*, vol. 10, no. 3, pp. 3066–3073, Jun. 2020, doi: 10.11591/ijece.v10i3.pp3066-3073.
[27] B. Sheng, W. Meng, C. Deng, and S. Xie, "Model based kinematic and dynamic simulation of 6-DOF upper-limb rehabilitation robot," in *2016 Asia-Pacific Conference on Intelligent Robot Systems (ACIRS)*, Jul. 2016, pp. 21–25, doi: 10.1109/ACIRS.2016.7556181.

BIOGRAPHIES OF AUTHORS

Imane Cheikh received the B.Eng. degree in electrical engineering from Hassania School of Public Works, Morocco, in 2020. She is a Ph.D. student in the Faculty of Sciences, Sidi Mohammed Ben Abdellah University of Morocco. Her research interests include nonlinear control for manipulator robots and fault-tolerant systems. She has authored scientific contributions, including a book chapter titled "The usefulness of digital twin in manipulator robot control," and a peer-reviewed conference paper "Robust sliding mode based on partial feedback linearization control for underactuated robot manipulator." In this work, she introduces an enhanced approach to virtual decomposition control by integrating a time-delay estimation technique, thereby making the method more robust and adaptive in the presence of actuator faults for robot manipulators. Her contributions demonstrate a strong commitment to advancing reliable and intelligent control methods in robotics. She can be contacted at email: imane.cheikh@usmba.ac.ma.

Khaoula Oulidi Omali holds a Ph.D. in robotics and electrical engineering from Sidi Mohammed Ben Abdellah University of Fes, Morocco. She is currently a professor in the National School for Computer Science and Systems Analysis, Mohammed V University. Her research interests include manipulator robots, fault-tolerant control, fault detection, smart industry, and internet of things, Industry 4.0. She can be contacted at email: khaoula.oulidi@ensias.um5.ac.ma.

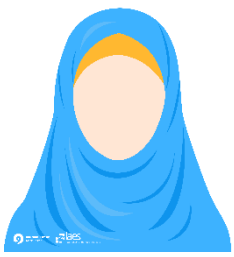

Hachmia Faqihi received her Ph.D. degree from the Mohammadia School of Engineering (EMI), Rabat, Morocco. She is currently a professor and researcher at Ibn Tofail University, Kenitra, Morocco. Her research interests include automation and robotics, cable-driven parallel robots, rehabilitation robotics, kinematic and dynamic modeling of multi-body systems, and advanced control strategies such as sliding-mode control and virtual decomposition control with time-delay estimation applied to cable-driven mechanisms. She can be contacted at: hachmia.faqihi@uit.ac.ma.

Mohammed Benbrahim received the B.Eng. degree in electromechanical engineering from the Higher National School of Mines in 1997 and the M.Sc. and Ph.D. degrees in automatic and industrial informatics from the Mohammadia School of Engineers in 2000 and 2007, respectively. Currently, he is a full professor at the Department of Physics, the director of the LIMAS laboratory and the program coordinator for the Master's program in Smart Industry at the Faculty of Sciences, Sidi Mohamed Ben Abdellah University. His research interests include robotics, automatic control, intelligent systems, predictive maintenance, modeling, and optimization. He can be contacted at email: mohammed.benbrahim@usmba.ac.ma.

Mohammed Nabil Kabbaj is a full professor at the Faculty of Sciences, University of Fez, where he is the Vice Dean in charge of Research and the Program Coordinator of the Mechatronics and Embedded Systems bachelor's program. His research interests include control engineering, fault detection, and diagnosis of complex systems. Before joining the University of Fez, he received a Ph.D. degree from the University of Perpignan in 2004 and was a postdoctoral researcher at LAAS-CNRS in Toulouse. He can be contacted at email: n.kabbai@usmba.ac.ma.